

# DC Micro-Grid Contactless Power Supply System with Active Load Detecting Control Method

Song Xu<sup>1, a</sup>, Seiji Hashimoto<sup>1, b</sup> and Wei Jiang<sup>2, c</sup>

<sup>1</sup>Division of Electronics and informatics, Gunma University, Kiryu, Gunma, Japan

<sup>2</sup>Department of Electrical Engineering, Yangzhou University, Yangzhou, China

<sup>a</sup><xusong0922@163.com>, <sup>b</sup><hashimotos@gunma-u.ac.jp>, <sup>c</sup><jiangwei@yzu.edu.cn>

**Keywords:** contactless power transfer, dc micro grid, active load detecting control.

**Abstract.** DC micro-grid is gaining an increasing attention in the field of power organization because of its high efficiency and intelligence in power organizing and using abilities. In this paper, a contactless power supply system for the mobile active load in the DC micro-grid with resonant network has been designed and analyzed. Moreover, for the energy saving purpose, the load detection function has been added to the transfer system. The theoretical analysis of the power transfer system and the resonant network is proposed. The simulation has been carried out in MATLAB/SIMULINK to test the control method. The experiment platform is built with a dsPIC controller, and then experiments are carried out to confirm the theoretical analysis and to verify the control efficiency of the load detecting control method.

## 1. Introduction

DC micro-grid is gaining more and more attention, because of the rapid development of new energy and distributed power generation technology. However, the isolated system protection between DC grid and the source load still need to be improved. The wireless power transfer technology provides a feasible way for the isolated protection. The technology uses the magnetic energy to transfer the electric power, and according to the way of power transfer, it can be divided into three parts: electromagnetic power transfer, resonance power transfer and radiation power transfer. Its benefits can be shortly concluded as no contact, safe and reliable, continuous power supply<sup>[1]-[7]</sup>.

This paper designed a contactless power supply system applied to the source load of DC micro-grid. The system is based on the principle of electromagnetic induction, using the series LC resonant tank to realize the non-contact power transmission<sup>[8]</sup>. Due to the characteristics of the source load, the power adjustment unit is designed to match the different voltage levels of the load. The system takes the DC micro-grid as the main power input, and in order to simulate the source load of the grid, the 48V battery is taken as the main load of the system. The system can realize the contactless power supply from the DC grid to the battery. In this paper, focusing on the load detecting function of the system, the combination of theory and experiment is used to evaluate the load detecting control method.

## 2. System Structure

The system frame and schematic diagram are shown in Fig. 1. The proposed system mainly includes five parts: input power, power conversion unit, resonant network unit, power adjustment unit and energy storage battery. The power conversion unit comprises the primary DC / AC conversion unit and the secondary AC / DC conversion unit. The resonant network is mainly composed of a series LC resonant network. Power adjustment unit is combined by the boost converter, taking 48V battery as the main load to simulate the source load of DC micro-grid.

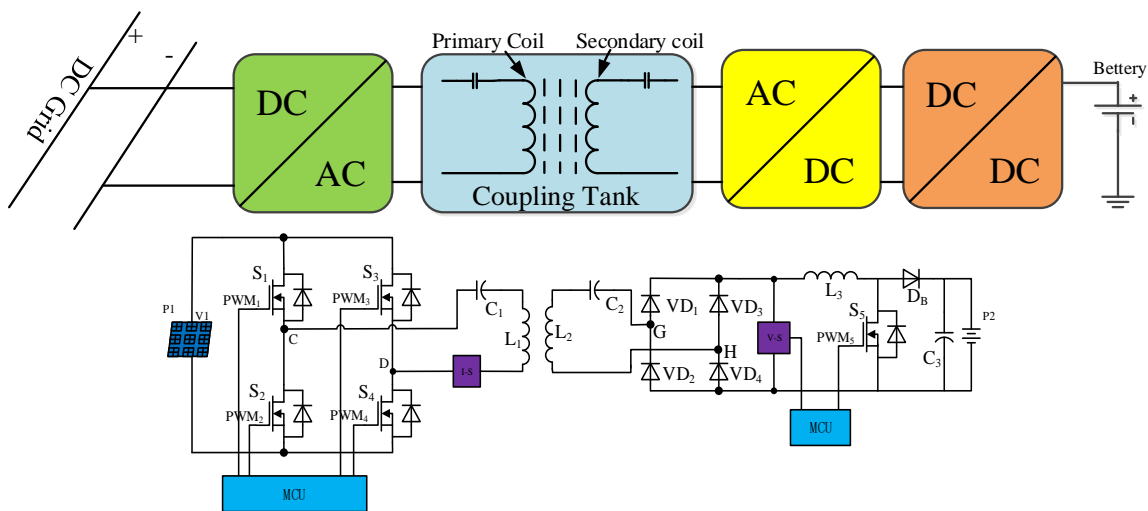


Fig. 1. System frame and schematic diagram

From the schematic diagram, the DC / AC converter unit in primary side and the AC/DC converter unit in secondary side both use the full bridge topology, and the resonant tank in both sides are the same LC series resonant net. The typical resonant network of both side of the system is shown in Fig. 2. Assuming that  $C_1$  is the primary resonant capacitor,  $L_1$  is the resonant inductance,  $C_2$  is the secondary resonant capacitor,  $L_2$  is the resonant inductance. In order to achieve the highest power transmission efficiency, the resonant frequency of the primary side  $f_1$  and secondary side  $f_2$  need to be same, as shown in Eq. (1).

$$f_1 = f_2 = \frac{1}{2\pi\sqrt{L_1C_1}} = \frac{1}{2\pi\sqrt{L_2C_2}} \tag{1}$$

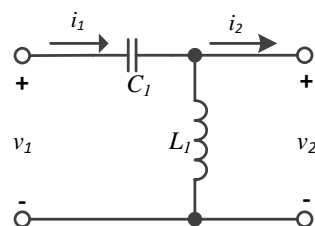


Fig.2. Typical LC series resonant net

### 3. System Analysis

#### 3.1 Resonant net efficiency analysis

The resonant net is applied in this system to realize the contactless power transfer. Fig. 3 shows the typical T-type equivalent circuit of the series resonant network topology.  $M$  is the mutual inductance between the primary coil and the secondary coil,  $R_1$  and  $R_2$  are the equivalent resistances of the primary and secondary coils. The ideal relationship between the system efficiency and the primary coil current  $I_1$ , secondary coil current  $I_2$  can be obtained by applying the AC small signal analysis method as shown in Eqs. (2) and (3).

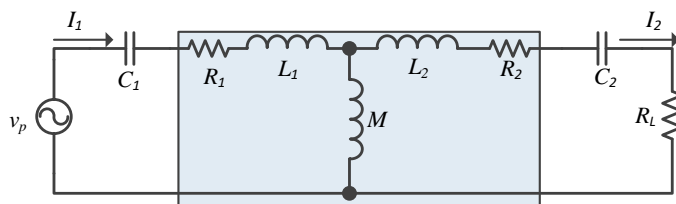


Fig. 3. Typical T-type equivalent circuit of series resonant network

The efficiency of the resonant network can be affected by the coupling coefficient between the primary coil and the secondary coil, hence it can also be influenced by the power factor. The ideal maximum efficiency of the resonant system can be obtained in Eq. (4).

$$\eta = \frac{I_2^2 R_L}{I_1^2 R_1 + I_2^2 R_2 + I_2^2 R_L} = \frac{R_L}{(R_L + R_2) \left( 1 + \frac{R_1(R_2 + R_L)}{\omega^2 M^2} \right)} \quad (2)$$

$$\frac{I_1}{I_2} = \frac{R_2 + R_L}{\omega_0 M} \quad (3)$$

$$\eta_{\max} = \frac{R_L}{R_2 + R_L} \quad (4)$$

From Eq. (4), the maximum efficiency of the system is almost independent of the load of the system. Since the equivalent resistant of the system load is much larger than the coil impedance, the system efficiency may not change when the system load changed. Therefore, the series resonant network efficiency is almost constant.

### 3.2 Inductance current analysis

The series resonant coupling tank is applied and the boost converter is used as the power adjustment unit, which can match the voltage level and make the system to have constant current in the resonant inductance. To analyze the characteristic of this system, the whole circuit topology can be equaled to a T-type simplified circuit as shown in Fig. 4.

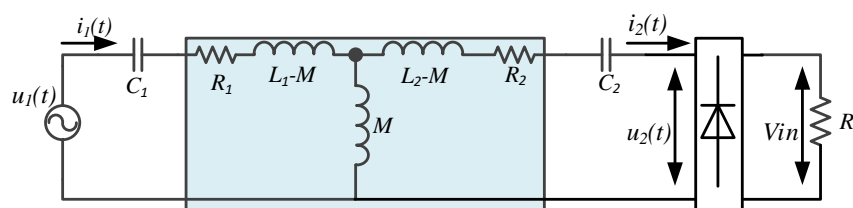


Fig. 4. Simplified T-type circuit

With this simplified circuit, assuming that  $k$  is the coupling coefficient between primary resonant inductance  $L_1$  and secondary resonant inductance  $L_2$ , the DC input voltage is  $E$ , the system angular frequency is  $\omega_0$ , the mutual inductance between the primary and secondary coils is  $M$ , as described in Eqs. (5) and (6)

$$\omega_0 = 2\pi\sqrt{L_1 L_2} \quad (5) \quad M = k\sqrt{L_1 L_2} \quad (6)$$

According to the principle of full bridge inverter, the relationship between  $u_1(t)$  and the input voltage  $E$  can be calculated as Eq. (7), also the relationship between  $u_2(t)$  and the input voltage of the Boost converter input voltage  $V_{in}$  can be calculated as Eq. (8).

$$u_1(t) = \frac{4E}{\pi} \sin(\omega_0 t) \quad (7) \quad u_2(t) = \frac{4V_m}{\pi} \sin\left(\omega_0 t + \frac{\pi}{2}\right) \quad (8)$$

According to Kirchhoff's law of voltage, the voltage identities of the primary side and secondary side are obtained as Eqs. (9) and (10)

$$i_1(t) \left( j\omega_0 L_1 + \frac{1}{j\omega_0 C_1} + R_1 \right) - j\omega_0 M i_2(t) = u_1(t) \quad (9)$$

$$i_2(t) \left( j\omega_0 L_2 + \frac{1}{j\omega_0 C_2} + R_2 \right) - j\omega_0 M i_1(t) = u_2(t) \quad (10)$$

When the system is working under the resonant frequency, due to the primary and secondary coil resistance  $R_1, R_2$  can be negligible, the system state meets Eq. (11)

$$j\omega_0 L_1 + \frac{1}{j\omega_0 C_1} = j\omega_0 L_2 + \frac{1}{j\omega_0 C_2} = 0 \quad (11)$$

So that we can get the current in the primary coil  $i_1(t)$  as Eq. (12) and the current in secondary coil  $i_2(t)$  as Eq. (13)

$$i_2(t) = -\frac{u_1(t)}{j\omega_0 M} \quad (12)$$

$$i_1(t) = \frac{4V_{in}}{\pi j \omega_0 M} \sin\left(\omega_0 t + \frac{\pi}{2}\right) \quad (13)$$

From the Eqs. (12) and (13), two main characteristics of the coupling system can be obtained. First, the current in the primary coil only can be influenced by the input voltage of the Boost converter, so if the voltage is controlled, the current in primary coil will be constant and independent of the DC input voltage. Second, the current in the secondary coil is only related to the DC voltage of the DC input. When the system is under the condition that the DC input voltage is constant, the current is not affected by the transmission power. These characteristics is named as the system coil current constant.

#### 4. Control System Design

In order to meet the load instability and save energy, the system should just work when there is load connected. That is, only when the load is accessed, the system is working continuously, if the load is absent, the system should be cut down and worked in the detecting mode, and no energy transmission is required. For this purpose, in the primary side of the system, the load detection control method was designed. The control block is shown in Fig. 5, where the maximum current in the primary coil is used to judge the load state, Moreover, the middle point sampling method is applied to get the maximum current.

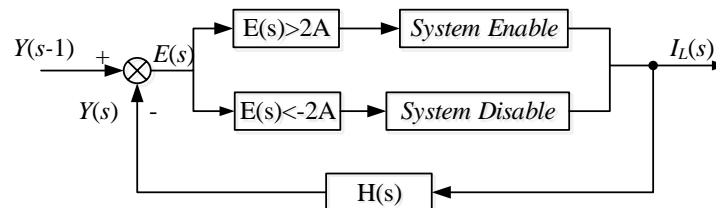


Fig.5. Load detection control block

In Fig. 4,  $Y(s)$  is the real-time output of the current sampling circuit,  $Y(s-1)$  is last cycle output of the sampling circuit,  $E(s)$  is the error between the last cycle sample and the current sample value,  $H(s)$  is the transfer function of the sampling circuit, and  $I_L(s)$  is the current in the primary coil.

According to the coupling theory, the maximum current error is set to 2 A as the control point of the system. So that, when  $E(s) > 2$  A, it can be seen that the load is connected, then system begin to work continuously and to transfer the power from DC micro-grid to the source load. When  $E(s) < -2$  A, it can be considered that the load has been cut off, then, the system changes the working model into detecting model. The detection state of the system is set to detect 20 ms per 1 s, so as to judge whether there is no load access, and control the system to achieve load detection control.

## 5. MATLAB/SIMULINK Simulation

According to the above analysis, the whole closed loop system is built in MATLAB / SIMULINK, mainly to verify the load detection function and the transfer power control. The main simulation circuit and each module are shown in Fig. 6. In this simulation, set the simulation time 0.6 s, and the load is connected at 0.3 s. After the load connection, the input voltage of the boost converter is controlled at 18 V. According to the theoretical analysis, before 0.3 s, the system should be working in the detection mode, after 0.3 s, the system should work continuously. The simulation result is shown in Fig. 7. the system works as the load detection state before 0.3 s, and works continuously and transfer power after 0.3 s.

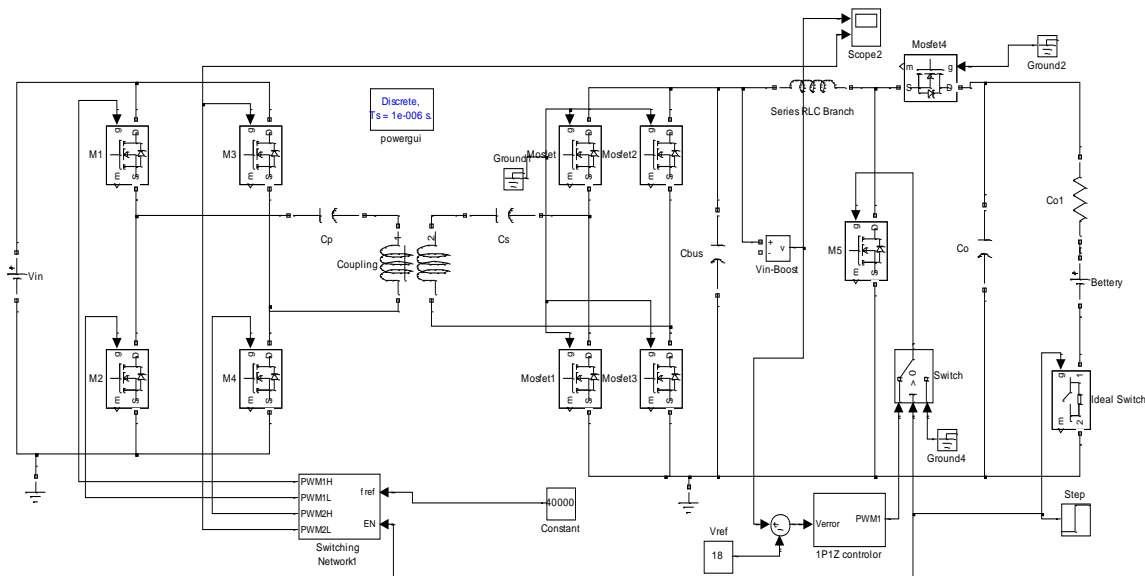


Fig. 6. MATLAB/SIMULINK simulation circuit

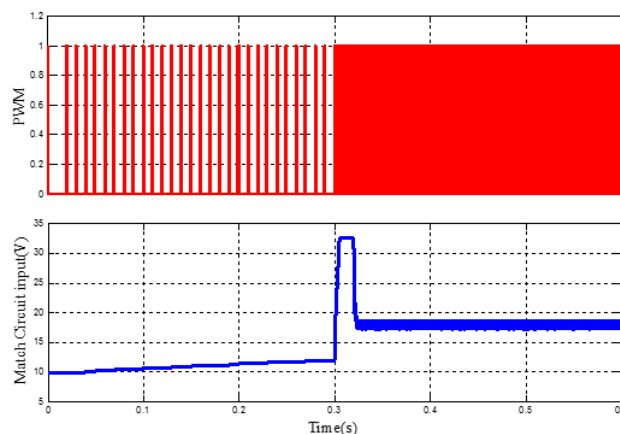


Fig. 7. Simulation result

## 6. Experiments and analysis

### 6.1 System configuration

An experimental platform with a 16-bit dsPIC as its controller is shown in Fig. 8. An adjustable bench power supply with 30 V and 20 A is selected as the input source to simulate the DC micro-grid. The load is a lead-acid battery pack rated at 48 V and 100 Ah. The major system parameters are listed in Table 1.

Table 1 System Parameters

| Component/<br>operation condition | Value              |
|-----------------------------------|--------------------|
| $L_1$                             | 26 $\mu\text{H}$   |
| $C_1$                             | 0.98 $\mu\text{F}$ |
| $L_2$                             | 28.5 $\mu\text{H}$ |
| $C_2$                             | 0.88 $\mu\text{F}$ |
| $f_s$                             | 31.5 kHz           |
| $T_s$                             | 100 $\mu\text{s}$  |

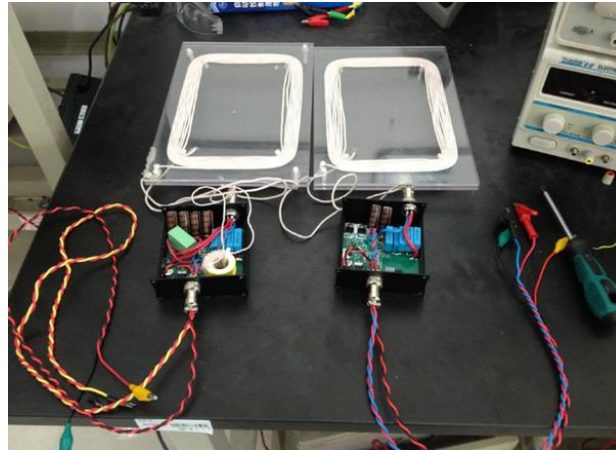


Fig. 8. Experiment platform

### 6.2 System start-up experiment

In order to get the highest transfer efficiency and the highest transfer power of this system, the switching frequency needs to be tested. According to the system parameter designed, the natural series resonant frequency of this system is  $f=31.5$  kHz, we scan around this frequency to determine the actual resonant frequency of this system. The suitable switching frequency is derived, taking the system safety into consideration.

Fig. 9 shows the waveform of the inverter output voltage and the current of the coil under the switching frequency of  $f_s=31.6$  kHz. From which we can see the phase of the voltage is a little ahead of the phase of the coil current, in this case the system works at the slight inductive mode. This mode is a safety and stable mode, so that we choose this switching frequency as the system frequency.

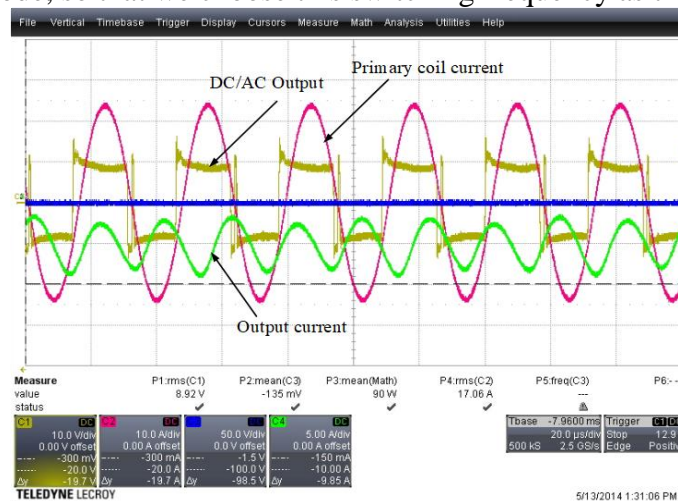


Fig. 9 Inverter output voltage and coil current with switching frequency  $f_s=31.6$  kHz

### 6.3 Power transfer efficiency experiment

In this experiment, in order to test the efficiency of the system, the input voltage of the DC/DC power adjustment unit (shown in Fig. 2) is varied to change the transfer power of this system. The airgap of the primary coil and the secondary coil is set to 70mm, and the input voltage of the DC/DC power adjustment unit is swept from 14 VDC to 21 VDC, to obtain the transfer power and the efficiency of the system, Figs. 10 and 11 show the relationship between the transfer power and input voltage, and the system efficiency and the input voltage of the DC/DC power adjustment unit, respectively.

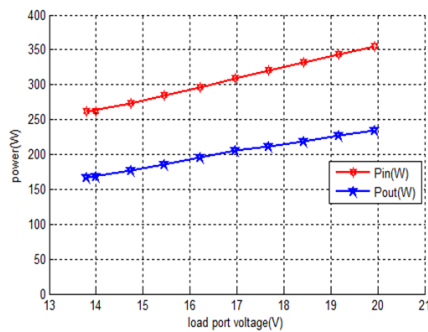


Fig. 10. Transfer power vs input voltage

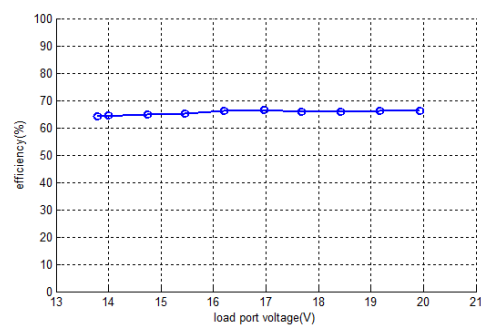


Fig. 11. System efficiency vs input voltage

From these figures, the transfer power increases when the input voltage of the DC/DC power adjustment voltage increases. However the system efficiency of the system almost keeps constant, which is in agreement with the analysis of the coupled system efficiency shown in Eq. (4).

### 6.4 Load detection experiment

The load detection is divided into three conditions: First, there is no load connected, the system just work under detecting model. Second, the system start-up with load connected, the system detecting the load and work continuously after start. Third, the system work at detecting model at beginning, when the load connected, the system changes into continuous working model.

Fig. 12 shows the first condition's experimental result. There is no load connected to the system, and the system was working at load detecting mode. The second condition's experimental result is shown in Fig. 13, where the system start-up with load already connected. After start-up, the system works continuously and transfers the power. The experimental result for last condition is shown in Fig. 14. As is said, the system works at detecting mode, and after the load connected, it changes into continuous working mode and transfer the power.

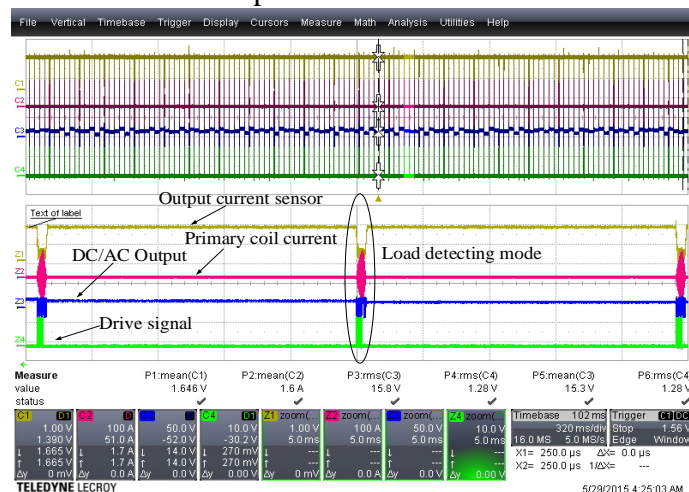


Fig. 12. First condition



Fig. 13. Second condition

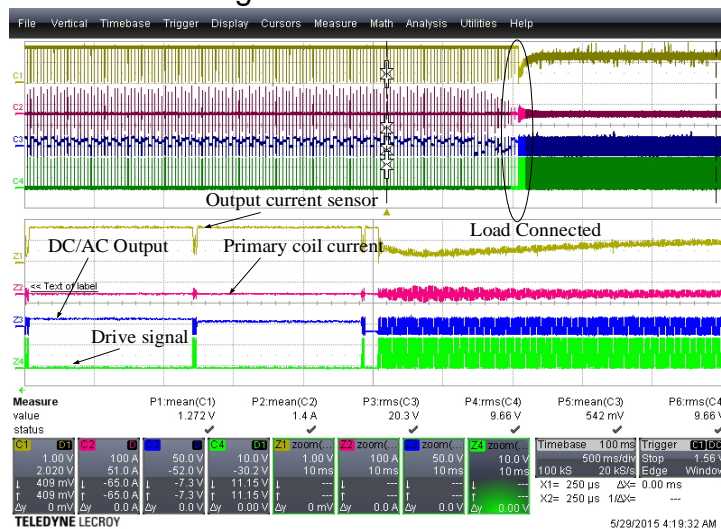


Fig. 14. Third condition

## 7. Conclusion

In this paper, a contactless power supply system applied to the source load of DC micro-grid has been proposed. The theoretical analysis in case of the resonant network of the system has been discussed. Focusing on the load detection function, an active load detecting control method has been proposed to realize this function. The whole system has been evaluated by simulations with MATLAB/SIMULINK, and the experiments have been carried out to verify the effectiveness of the load detecting control method. Moreover, the theoretical analysis of the results also has been investigated.

## References

- [1] M. Budhia and G. A. Covic and J. T. Boys, "Design and optimization of circular magnetic structures for lumped inductive power transfer systems," *IEEE Trans. Power Electron.*, vol. 26, no. 11, pp. 3096-3108, 2011.

- [2] C. Wang and G. A. Covic and O. H. Stielau, "Power transfer capability and bifurcation phenomena of loosely coupled inductive power transfer systems," *IEEE Trans. Ind. Electron.*, vol. 51, no. 1, pp. 148-157, 2004.
- [3] C. J. Chen, and T. H. Chu and C. L. Lin and Z. C. Jou, "A study of loosely coupled coils for wireless power transfer," *IEEE Trans. Circuits Syst.*, vol. 57, no. 71, pp. 536-540, 2010.
- [4] O. H. Stielau and G. A. Covic, "Design of loosely coupled inductive power transfer systems," in *Proc. Int. Conf. Power Syst. Technol.*, vol. 1, pp. 85-90, 2000.
- [5] B. Klontz, K.W., D. Divan, D. Novotny, R. Lorenz, Contactless Power Delivery System for Mining Applications, *IEEE Transactions on Industry Applications*, vol.31, no. 1, pp. 27-35, Jan./Feb. 1995.
- [6] M. L. G. Kissin, H. Hao and G. A. Covic, "A practical multiphase IPT system for AGV and roadway applications," in *IEEE Energy Conversion Congress and Exposition*, pp. 1844–1850 , 2010.
- [7] Y. Jang and M. Jovanovic, "A contactless electrical energy transmission system for portable-telephone battery chargers", *IEEE Transactions on Industrial Electronics*, vol. 50, no. 3, pp. 520-527, 2003.
- [8] Song Xu, S. Hashimoto, Wei Jiang, "DC Micro-Grid Contactless Power Supply System with Load Detecting Control Method," *International Conference on Mechanical, Electrical and Medical Intelligent System 2017 (ICMEMIS2017)*, ID:I08-06, 2017.